

Cite this: *CrystEngComm*, 2012, **14**, 1216

www.rsc.org/crystengcomm

Two-dimensional frameworks built from Single-Molecule Magnets†

Athanasios D. Katsenis,^a Ross Inglis,^b Alessandro Prescimone,^b Euan K. Brechin^{*b} and Giannis S. Papaefstathiou^{*a}

Received 16th November 2011, Accepted 16th December 2011

DOI: 10.1039/c2ce06536c

Fine tuning the Mn/salicylaldehyde/trimesic acid reaction conditions leads to the formation of a regular 2D net held together by dative bonds and to a non-regular 2D net stabilised by both dative and hydrogen bonds. Both networks are built from [Mn₆] Single-Molecule Magnets.

Since it has been established that the physical properties of crystalline molecular materials can be influenced by crystal packing effects and intermolecular interactions (*e.g.* hydrogen bonding, $\pi \cdots \pi$ interactions, *etc.*), we and others have been investigating how to manipulate the magnetic properties of Single-Molecule Magnets (SMMs) in the solid state by modulating their surroundings.¹ To this end, we recently exploited certain members of a family of hexanuclear, [Mn₆], and trinuclear, [Mn₃], Mn^{III} complexes of general formulae [Mn^{III}₆O₂(R-sao)₆(O₂CR)₂(L)₄₋₆] and [Mn^{III}₃O(R-sao)₃(X)(L)₃] (saoH₂ = salicylaldehyde; R = H, Me, Et, *etc.*; X = RCO₂⁻, ClO₄⁻; L = solvent)^{2,3} as building blocks for constructing discrete and infinite supramolecular architectures with the use of both bis-pyridyl⁴ and bis-carboxylate⁵ type ligands. Both types of bridging ligands resulted in, among others, coordination polymers built from either [Mn₃] or [Mn₆] clusters. The bis-pyridyl type ligands gave rise to both one- (1D) and two-dimensional (2D) coordination polymers based on [Mn₃] SMMs while the bis-carboxylate ligands resulted in 1D coordination polymers incorporating [Mn₆] SMMs.^{4,5}

Having in mind that the incorporation of bis-carboxylate ligands resulted in polymeric species where the [Mn₆] clusters retained their single molecule behaviour, we sought to construct higher dimensionality coordination polymers (*i.e.* 2D or 3D) built from [Mn₆] SMMs and polycarboxylate ligands. For this purpose, we incorporated 1,3,5-benzene-tricarboxylic acid (trimesic acid, tmaH₃) into blends of manganese/saoH₂ reaction mixtures to isolate the 1D coordination polymer [Mn₆O₂(sao)₆(tmaH)(MeOH)_{8.5}(H₂O)_{0.5}]·(MeOH)_{0.75}(H₂O)_{0.125} **1**·(MeOH)_{0.75}(H₂O)_{0.125} and the 2D

coordination polymer [Mn₆O₂(sao)₆(tma)_{0.66}(MeOH)_{3.33}(H₂O)_{1.33}]·(MeOH)_{4.46}(H₂O) **2**·(MeOH)_{4.46}(H₂O). Both polymers are constructed from [Mn₆] SMM building blocks. Besides the efforts to intentionally link SMMs or magnetically interesting clusters, higher dimensionality (*i.e.* 2D, 3D) polymers are scarce.⁶ Complex **2** represents a rare 2D framework constructed intentionally from SMM building blocks.

Although it is possible to employ pre-formed [Mn₆] and [Mn₃] species as starting materials for the synthesis of polymeric materials [they are solution stable as gauged by NMR, mass spectrometry and solution SQUID magnetometry⁷], it is much more efficient to simply perform the reactions *in situ*. The Mn(ClO₄)₂·6H₂O/saoH₂/tmaH₃/base reaction blend is however very sensitive to reaction conditions and indeed it produces different complexes depending on the order of addition of the reagents. The 1D coordination polymer **1** is produced when tmaH₃ is added into an alcoholic solution containing Mn(ClO₄)₂·6H₂O/saoH₂/MeONa, while the 2D coordination polymer **2** is formed when MeONa was added into an alcoholic solution containing Mn(ClO₄)₂·6H₂O/saoH₂/tmaH₃. Complex **1** was isolated serendipitously during our efforts to synthesise the targeted 2D coordination polymer **2**.

Complex **1** (Fig. 1) crystallises in the triclinic space group $P\bar{1}$.‡ The asymmetric unit consists of two tmaH²⁻ anions, one [Mn^{III}₆] and two [Mn^{III}₃] units.† In effect, there are two crystallographically independent [Mn₆] clusters, namely [Mn₆]_A and [Mn₆]_B, repeating along the chain of **1**. Each [Mn₆] unit consists of two off-set, stacked [Mn^{III}₃O(sao)₃]⁺ triangles linked by two oximate O-atoms, while one phenolato O-atom bridges between the [Mn₃] subunits in [Mn₆]_A. Four sao²⁻ ligands bridge along the edges of the [Mn₃] subunits in a $\mu_3:\eta^1:\eta^1:\eta^2$ fashion, one in a $\mu_3:\eta^2:\eta^1:\eta^1$ fashion while the remaining seven sao²⁻ ligands adopt the $\mu:\eta^1:\eta^1:\eta^1$ coordination mode. Ten out of the twelve crystallographically independent Mn^{III} atoms are in (axially) elongated octahedral environments with one Mn^{III} in each of the [Mn₆] clusters being five-coordinate and in a square pyramidal environment. Nine MeOH molecules (one is 50% disordered with a H₂O molecule) occupy the Jahn Teller positions on the Mn^{III} ions, with the remaining sites coordinated by carboxylato O-atoms from the two crystallographically independent tmaH²⁻ ligands. These ligands adopt the $\mu_4:\eta^1:\eta^1:\eta^1:\eta^1$ and $\mu_3:\eta^1:\eta^1:\eta^1$ coordination modes, respectively. The Mn–N–O–Mn torsion angles for [Mn₆]_A are 32.55° for Mn4–N–O–Mn5, 38.22° for Mn5–N–O–Mn6, 21.47° for Mn6–N–O–Mn4, 41.83° for Mn7–N–O–Mn8, 12.25° for Mn8–N–O–Mn9 and 30.13° for Mn9–N–O–Mn7. For [Mn₆]_B the corresponding

^aLaboratory of Inorganic Chemistry, Department of Chemistry, National and Kapodistrian University of Athens, Panepistimiopolis, 157 01 Zografou, Greece. E-mail: gspapaef@chem.uoa.gr; Fax: +30 210-727-4782; Tel: +30 210-727-4840

^bEaStCHEM School of Chemistry, The University of Edinburgh, West Mains Road, Edinburgh, EH9 3JJ, UK. E-mail: ebrechin@staffmail.ed.ac.uk; Tel: +44 131 650 7545

† Electronic supplementary information (ESI) available: CIF files of complexes **1** and **2**, figures and experimental details. See DOI: 10.1039/c2ce06536c

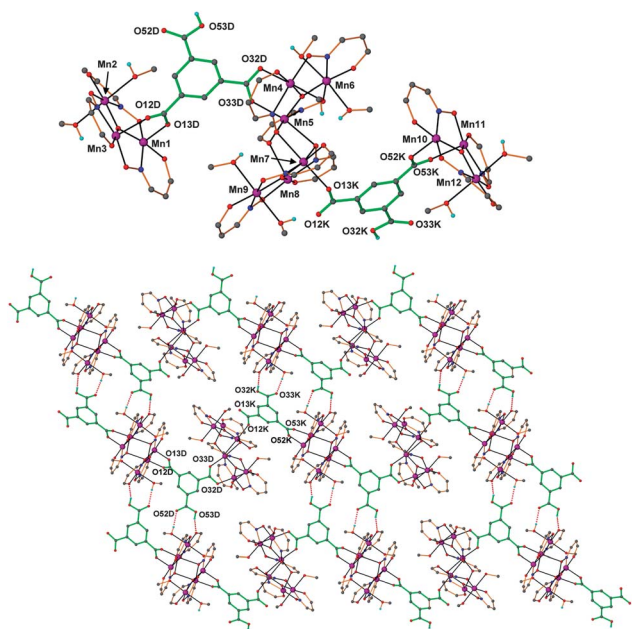


Fig. 1 (top) The asymmetric unit of complex **1**. (bottom) The hydrogen-bonded chains of complex **1** creating a non-regular 2D framework. Most hydrogen atoms and some carbon atoms of the sao^{2-} ligands have been omitted for clarity. Colour code: Mn: purple, O: red, N: blue, C: grey, and H: cyan.

angles are 18.00° for Mn1–N–O–Mn2, 8.18° for Mn2–N–O–Mn3, 13.44° for Mn3–N–O–Mn1, 15.99° for Mn10–N–O–Mn11, 9.05° for Mn11–N–O–Mn12 and 18.44° for Mn12–N–O–Mn10.

The chains of **1** are arranged in parallel, with the free carboxylic acid groups of the tmaH^{2-} ligands able to donate a hydrogen bond to a phenolato O-atom and accept a hydrogen bond from a neighbouring coordinated MeOH molecule, thus bridging between chains to create a 2D non-regular network (Fig. 1) with vertex symbol (4.6⁺;4.6.4.6). The tmaH^{2-} ligands and the $[\text{Mn}_6]_{\text{B}}$ clusters serve as 3- and 4-connected nodes within the 2D network, respectively, with $[\text{Mn}_6]_{\text{A}}$ simply bridging between the tmaH^{2-} ligands.

Complex **2** also crystallises in the triclinic space group $P\bar{1}$.[‡] The asymmetric unit consists of one tma^{3-} anion and three $[\text{Mn}^{\text{III}}_3\text{O}(\text{sao})_3]^+$ subunits (Fig. 2).[†] This arrangement gives rise to three crystallographically independent $[\text{Mn}_6]$ clusters, with each sitting on an inversion centre. Two off-set stacked $[\text{Mn}^{\text{III}}_3\text{O}(\text{sao})_3]^+$ triangles linked by two oximate O-atoms create each $[\text{Mn}_6]$ cluster. Therefore, four sao^{2-} ligands bridge along the edges of the $[\text{Mn}_3]$ subunits in a $\mu_3:\eta^1:\eta^1:\eta^1$ fashion, while two sao^{2-} ligands adopt the $\mu_3:\eta^1:\eta^1:\eta^2$ coordination mode. Two Mn^{III} ions in each $[\text{Mn}_6]$ are five-coordinate in a square pyramidal environment while the remaining four Mn^{III} ions are in (axially) elongated octahedral environments. Ten MeOH and four H_2O molecules, ten carboxylate O-atoms from the tma^{3-} ligands and six oximate O-atoms from the sao^{2-} ligands occupy the Jahn Teller positions on the Mn^{III} ions. The tma^{3-} ligand bridge five Mn^{III} ions, from three different $[\text{Mn}_6]$ clusters, adopting the $\mu_5:\eta^1:\eta^1:\eta^1:\eta^1:\eta^1$ coordination mode. The Mn–N–O–Mn torsion angles are 9.45° for Mn1–N–O–Mn2, 1.81° for Mn2–N–O–Mn3 and 31.37° for Mn3–N–O–Mn1 for the first $[\text{Mn}_6]$, 24.64° for Mn4–N–O–Mn5, 14.67° for Mn5–N–O–Mn6 and 18.22° for Mn6–N–O–Mn4 for the second $[\text{Mn}_6]$ and 2.33° for Mn7–N–O–Mn8, 29.81° for Mn8–N–O–Mn9 and 22.60° for Mn9–N–O–Mn7 for the third $[\text{Mn}_6]$.

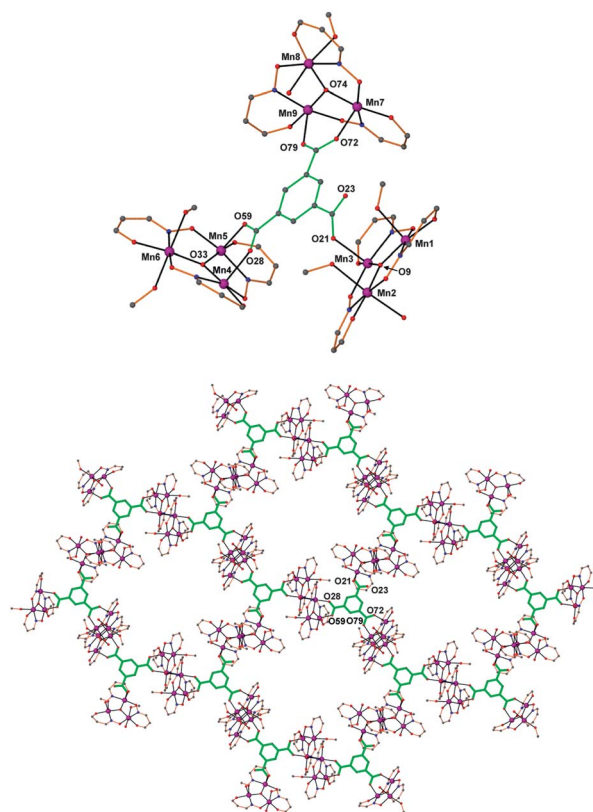


Fig. 2 (top) The asymmetric unit of complex **2**. (bottom) The 2D framework of complex **2**. All hydrogen atoms and many carbon atoms of the sao^{2-} ligands have been omitted for clarity. Colour code as in Fig. 1.

The $[\text{Mn}_6]$ clusters and the tma^{3-} ligands assemble to create a regular 2D network with a (6,3) topology, commonly known as a honeycomb, with the tma^{3-} ligands serving as 3-connected nodes and the $[\text{Mn}_6]$ clusters as the spacers (Fig. 2).

Previous studies of molecular salicylaldoxime-based $[\text{Mn}^{\text{III}}_6]$ and $[\text{Mn}^{\text{III}}_3]$ clusters have shown that their magnetic behaviour is strongly correlated to small geometrical changes. Specifically, the sign and magnitude of the exchange (J) between neighbouring Mn^{III} ions is dependent on the Mn–N–O–Mn torsion angle. Unfortunately the presence of more than one crystallographically independent $[\text{Mn}_6]$ in the crystal structures of both **1** and **2**, which possess different geometries, precludes a detailed *quantitative* analysis of the magnetic behaviour.

Solid state dc magnetic susceptibility data for **1** and **2** were recorded between 275 and 5 K in an applied field of 0.1 T. The plots of $\chi_{\text{M}}T$ versus T for **1** and **2** are shown in Fig. S1[†]. The $\chi_{\text{M}}T$ products at 275 K are 16.54 and 14.95 $\text{cm}^3 \text{mol}^{-1} \text{K}$ for **1** and **2**, respectively, close to the spin-only ($g = 2$) value of 18 $\text{cm}^3 \text{mol}^{-1} \text{K}$ expected for a $[\text{Mn}_6]$ unit comprising six high spin Mn^{III} ions. The $\chi_{\text{M}}T$ values for both complexes remain approximately constant as the temperature is lowered, before dropping more rapidly at temperatures below 125 K. Thereafter, the $\chi_{\text{M}}T$ value of complex **1** decreases constantly to reach a value of 9.1 $\text{cm}^3 \text{mol}^{-1} \text{K}$ at 5 K, while that of complex **2** decreases to a value of ~ 8.0 $\text{cm}^3 \text{mol}^{-1} \text{K}$ at 20 K and then plateaus to 5 K. The decrease of the $\chi_{\text{M}}T$ product upon cooling to smaller but non-zero values is consistent with the presence of both antiferromagnetic and ferromagnetic interactions between the Mn^{III} ions with the

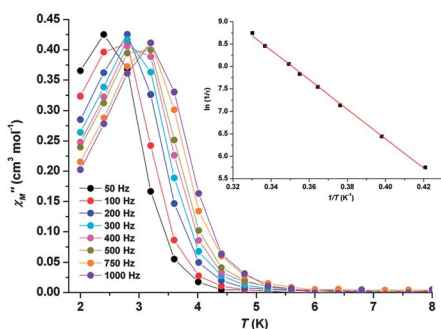


Fig. 3 Plot of χ'' versus T for complex **1** at the indicated temperature and frequency ranges. Inset: Arrhenius plot constructed from the χ'' data to afford $\tau_0 = 3.3 \times 10^{-9}$ s and $U_{\text{eff}} \approx 33$ K.

low-temperature values indicating $S \approx 4$ spin ground states for the $[\text{Mn}^{\text{III}}_6]$ units in both complexes. Indeed we note that the $\chi_{\text{M}}T$ behaviour for **1** and **2** is very similar to that observed for previously reported and magnetically isolated $[\text{Mn}^{\text{III}}_6]$ complexes with $S = 4$ spin ground states. For comparison we include in Fig. S1† the data for $[\text{Mn}_6\text{O}_2(\text{sao})_6(\text{ketoacetate})_2(\text{EtOH})_2(\text{H}_2\text{O})_2]$ (**3**) and $[\text{Mn}_6\text{O}_2(\text{sao})_6(1\text{-Me-cyclohex})_2(\text{MeOH})_4]$ (**4**) from ref. 3b which contain $[\text{Mn}_6]$ with similar Mn–N–O–Mn torsion angles. In order to investigate the possibility of long range antiferromagnetism we performed zero field ac susceptibility measurements on **1** and **2** in the 1.8–10 K temperature range with a 3.5 G ac field oscillating at frequencies ranging from 50–1000 Hz (Fig. 3). A cusp in the real component χ' (Fig. S3†) is accompanied by a non-zero imaginary component χ'' at ~ 3 K. The maxima for both are strongly frequency dependent, suggesting super-paramagnetic blocking of the magnetisation. Arrhenius plots (inset of Fig. 3) constructed from the χ'' data afford $\tau_0 = 3.3 \times 10^{-9}$ s and $U_{\text{eff}} = 32.84$ K (22.82 cm^{-1}) for **1**, and $\tau_0 = 5.6 \times 10^{-8}$ s and $U_{\text{eff}} = 24.54$ K (17.05 cm^{-1}) for **2**. The presence of significant inter- $[\text{Mn}_6]$ interactions would be expected to slow down the spin dynamics at low temperatures and this would be manifested in a smaller frequency shift, k . Using the average values of blocking temperatures (T_{B}) of 2.70 K for **1** and 2.69 K for **2**, the frequency shift of T_{B} is calculated as $k = \Delta T_{\text{B}} / (T_{\text{B}} \Delta \log f)$, where ΔT_{B} is the change in T_{B} for the given change in frequency $\Delta \log f$, where $\Delta \log f = 1.30$ for both complexes. This provides values of 0.19 and 0.24 for **1** and **2**, respectively, which are within the range expected for super-paramagnets and close to those reported for molecular $[\text{Mn}_6]$ complexes. This suggests that the relaxation is in accordance with SMM behaviour, and is not attributed to long range interactions mediated through the polycarboxylate ligands.

To conclude, we presented two new coordination polymers built from $[\text{Mn}_6]$ clusters and trimesate anions. The first polymer conforms to a non-regular 2D net held by both dative and hydrogen bonds, while the second adopts a regular 2D net held together exclusively by dative bonds. Both polymers consist of magnetically isolated $[\text{Mn}_6]$ SMMs with $S \approx 4$ ground states. We continue exploiting $[\text{Mn}_6]$ SMMs as starting materials for the construction of polymeric

magnetic materials with the next stage being the introduction of added functionality through the presence of redox-active or radical linker ligands which might enable [stronger] communication between the cluster building blocks.

Notes and references

† Crystal data for **1**: $\text{C}_{224}\text{H}_{220}\text{Mn}_{24}\text{N}_{24}\text{O}_{101.50}$, $M = 6190.80$, triclinic, $a = 12.5838(4)$ Å, $b = 19.5656(5)$ Å, $c = 25.6050(6)$ Å, $\alpha = 99.792(2)^\circ$, $\beta = 90.436(2)^\circ$, $\gamma = 97.756(2)^\circ$, $V = 6152.5(3)$ Å³, $T = 100(2)$ K, space group $P\bar{1}$, $Z = 1$, 121 047 reflections measured, 24 245 independent reflections ($R_{\text{int}} = 0.1296$). The final R_1 values were 0.0674 ($I > 2\sigma(I)$). The final $wR(F^2)$ values were 0.1494 ($I > 2\sigma(I)$). The final R_1 values were 0.1601 (all data). The final $wR(F^2)$ values were 0.1759 (all data). Crystal data for **2**: $\text{C}_{83.70}\text{H}_{100.80}\text{Mn}_9\text{N}_9\text{O}_{42.20}$, $M = 2402.52$, triclinic, $a = 14.7534(4)$ Å, $b = 16.3686(4)$ Å, $c = 22.2983(6)$ Å, $\alpha = 101.659(2)^\circ$, $\beta = 101.396(2)^\circ$, $\gamma = 96.649(2)^\circ$, $V = 5101.3(3)$ Å³, $T = 100$ K, space group $P\bar{1}$, $Z = 2$, 42 686 reflections measured, 19 808 independent reflections ($R_{\text{int}} = 0.055$). The final R_1 values were 0.0744 ($I > 2\sigma(I)$). The final $wR(F^2)$ values were 0.1160 (all data). The final $wR(F^2)$ values were 0.0128 ($I > 2\sigma(I)$). The final R_1 values were 0.1160 (all data). The final $wR(F^2)$ values were 0.0128 (all data).

- (a) R. Inglis, G. S. Papaefstathiou, W. Wernsdorfer and E. K. Brechin, *Aust. J. Chem.*, 2009, **62**, 1108; (b) S. Hill, R. S. Edwards, N. Aliaga-Alcalde and G. Christou, *Science*, 2003, **302**, 1015; (c) H. Miyasaka and M. Yamashita, *Dalton Trans.*, 2007, 399; (d) G. Novitchi, W. Wernsdorfer, L. F. Chibotaru, J. P. Costes, C. E. Anson and A. K. Powell, *Angew. Chem., Int. Ed.*, 2009, **48**, 1614; (e) W. Wernsdorfer, N. Aliaga-Alcalde, D. N. Hendrickson and G. Christou, *Nature*, 2002, **416**, 406.
- (a) R. Inglis, S. M. Taylor, L. F. Jones, G. S. Papaefstathiou, S. P. Perlepes, S. Datta, S. Hill, W. Wernsdorfer and E. K. Brechin, *Dalton Trans.*, 2009, 9157; (b) C. J. Milios, R. Inglis, L. F. Jones, A. Prescimone, S. Parsons, W. Wernsdorfer and E. K. Brechin, *Dalton Trans.*, 2009, 2812.
- (a) C. J. Milios, R. Inglis, A. Vinslava, R. Bagai, W. Wernsdorfer, S. Parsons, S. P. Perlepes, G. Christou and E. K. Brechin, *J. Am. Chem. Soc.*, 2007, **129**, 12505; (b) R. Inglis, L. F. Jones, C. J. Milios, S. Datta, A. Collins, S. Parsons, W. Wernsdorfer, S. Hill, S. P. Perlepes, S. Piligkos and E. K. Brechin, *Dalton Trans.*, 2009, 3403.
- (a) C. C. Stoumpos, R. Inglis, G. Karotsis, L. F. Jones, A. Collins, S. Parsons, C. J. Milios, G. S. Papaefstathiou and E. K. Brechin, *Cryst. Growth Des.*, 2009, **9**, 24; (b) R. Inglis, A. D. Katsenis, A. Collins, F. White, C. J. Milios, G. S. Papaefstathiou and E. K. Brechin, *CrystEngComm*, 2009, **11**, 2117.
- L. F. Jones, A. Prescimone, M. Evangelisti and E. K. Brechin, *Chem. Commun.*, 2009, 2023.
- For 2D and 3D frameworks built from SMMs see: (a) G. Wu, J. Huang, L. Sun, J. Bai, G. Li, E. Cremades, E. Ruiz, R. Clérac and S. Qiu, *Inorg. Chem.*, 2011, **50**, 8580; (b) O. Roubeau and R. Clérac, *Eur. J. Inorg. Chem.*, 2008, 4325; (c) I.-R. Jeon, R. Ababei, L. Lecren, Y.-G. Li, W. Wernsdorfer, O. Roubeau, C. Mathoniere and R. Clérac, *Dalton Trans.*, 2010, **39**, 4744; (d) Y.-L. Bai, J. Tao, R.-B. Huang and L.-S. Zheng, *Angew. Chem., Int. Ed.*, 2008, **47**, 5344; (e) E. E. Moushi, T. C. Stamatatos, W. Wernsdorfer, V. Nastopoulos, G. Christou and A. J. Tasiopoulos, *Angew. Chem., Int. Ed.*, 2006, **45**, 7722; (f) M. Murugesu, R. Clérac, W. Wernsdorfer, C. E. Anson and A. K. Powell, *Angew. Chem., Int. Ed.*, 2005, **44**, 6678; (g) H. Miyasaka, K. Nakata, K. Sugiura, M. Yamashita and R. Clérac, *Angew. Chem., Int. Ed.*, 2004, **43**, 707; (h) H. Miyasaka, K. Nakata, L. Lecren, C. Coulon, Y. Nakazawa, T. Fujisaki, K. Sugiura, M. Yamashita and R. Clérac, *J. Am. Chem. Soc.*, 2006, **128**, 3770.
- R. Inglis, J. Bendix, T. Brock-Nannestad, H. Weihe, E. K. Brechin and S. Piligkos, *Chem. Sci.*, 2010, **1**, 631.